Inorganic Chemistry

Article

pubs.acs.org/IC

Thymines in Single-Stranded Oligonucleotides and G-Quadruplex DNA Are Competitive with Guanines for Binding to an Organoruthenium Anticancer Complex

Kui Wu,[†,‡,⊥] Suyan Liu,[†,‡,⊥] Qun Luo,[†,‡] Wenbing Hu,[†,‡] Xianchan Li,[†,‡] Fuyi Wang,*[,†,‡] Renhui Zheng,[†,§] Jie Cui,[†] Peter J. Sadler,*[,∥] Junfeng Xiang,[†] Qiang Shi,[†,§] and Shaoxiang Xiong[†,‡]

[†]Beijing National Laboratory for Molecular Sciences, Institute of Chemistry, Chinese Academy of Sciences, Beijing 100190, P. R. China

[‡]CAS Key Laboratory of Analytical Chemistry for Living Biosystems, Beijing Centre for Mass Spectrometry, Beijing 100190, P. R. China

[§]State Key Laboratory for Structural Chemistry of Unstable and Stable Species, Beijing 100190, P. R. China

[∥]Department of Chemistry, University of Warwick, Gibbet Hill Road, Coventry CV4 7AL, United Kingdom

Supporting Information

ABSTRACT: Organometallic ruthenium(II) complexes $[(\eta^6\text{-arene})\text{Ru(en)Cl}]^+$ (arene = e.g., biphenyl (**1**), dihydrophenanthrene, tetrahydroanthracene) show promising anticancer activity both in vitro and in vivo and are cytotoxic to cisplatin-resistant cancer cells, implying that these monofunctional complexes have a different mechanism of action from that of bifunctional cisplatin. We demonstrate here that complex **1** binds selectively to the guanine base in the 15-mer single-stranded oligodeoxynucleotides (ODNs) 5′-CTCTCT$X_7G_8Y_9$CTTCTC-3′ [X = Y = T; X = C, Y = A; X = A, Y = T; X = T, Y = A] to form thermodynamically stable adducts, but thymine bases (T_7/T_{11} or T_6/T_{11}) compete kinetically with guanine for binding to **1**. The T-bound monoruthenated species eventually convert to diruthenated products via a second step of binding at G or/and to G-bound monoruthenated species through dissociation of the diruthenated adducts. Complex **1** was further shown to bind preferentially to the middle T in a sequence rather than to a T near the terminus and favor coordination to a 5′-T compared to a 3′-T. Interestingly, the T bases in the human telomeric G-quadruplex sequence (5′-AGGGTTAGGGTTAGGGTTAGGG-3′) were found to be more competitive both kinetically and thermodynamically with G bases for binding to **1**. These results suggest that thymine bases play a unique role in the pathways of ruthenation of DNA by organoruthenium anticancer complexes and illustrate that kinetic studies can provide new insight into the mechanism of action of metallodrugs in addition to study of the structures and functions of the thermodynamically stable end products.

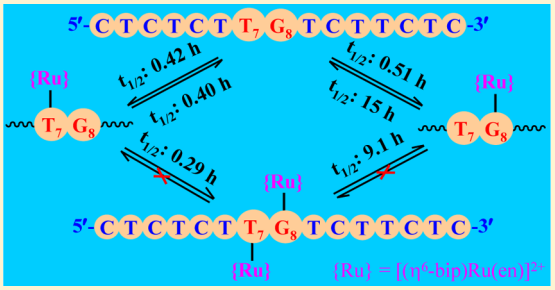

INTRODUCTION

The serendipitously discovered anticancer drug cisplatin has now been widely used in the chemotherapy of several forms of cancer,[1,2] especially for testicular cancer with more than a 90% cure rate.[3] It is generally accepted that DNA is the primary target of cisplatin,[4−6] with approximately 65% 1,2-d(GpG) and 25% 1,2-d(ApG) intrastrand cross-links as major adducts,[7−9] which are recognized by HMGB proteins, circumventing nucleotide excision repair (NER) and leading to cell apoptosis.[4−6] However, cisplatin therapy suffers from two main problems: inherent and acquired resistance and severe side effects.[5,9,10] Consequently, the quest for alternative drugs which increase selectivity for cancer cells and reduce side effects is currently attracting much attention.[1,9,11−17]

Organometallic compounds, with a great structural variety and diverse stereochemistry, have recently been found to be promising anticancer drug candidates.[17−21] Among these, organometallic ruthenium(II) complexes $[(\eta^6\text{-arene})\text{Ru(XY)Z}]^+$ exhibit anticancer activity both in vitro and in vivo.[22−25] Complexes with XY = ethylenediamine (en) and Z = Cl, a monodentate leaving group,[24−26] are cytotoxic to cisplatin-resistant cancer cells.[22,24,26] This suggests that the monofunctional complexes have a different mechanism of action from that of bifunctional cisplatin[4−6] and those of the Ru(III) anticancer complexes (ImH)[*trans*-$RuCl_4Im(Me_2SO)$] (Im = imidazole, NAMI-A) and (IndH)[*trans*-$RuCl_4(Ind)_2$] (Ind = indazole, KP1019) which are currently undergoing clinical trials.[11,27−29] The cytotoxicity of the group of complexes $[(\eta^6\text{-arene})\text{Ru(en)Cl}]^+$ increases with the size of coordinated arene in the following order: benzene (ben) < *p*-cymene (*p*-cym) < biphenyl (bip) < dihydroanthracene (dha) < dihydrophenan-

Received: June 25, 2013
Published: September 11, 2013

   dx.doi.org/10.1021/ic401606v | *Inorg. Chem.* 2013, 52, 11332−11342

threne (dhpa) ≈ tetrahydroanthracene (tha).[22,26] The activity of biphenyl complexes against the human ovarian cancer cell line A2780 is comparable to that of carboplatin, and that of the tetrahydroanthrancene complexes approaches that of cisplatin.[22,24]

As for cisplatin,[4−6] DNA is thought to be a potential target for the Ru^{II} arene complexes.[23,30−36] These complexes with arene = ben, *p*-cym, bip, dha, or tha bind preferentially to N7 of guanosine, and reaction of complex $[(\eta^6\text{-biphenyl})Ru(en)Cl]^+$ (**1**, Chart 1) with 5′-GMP and either 5′-AMP or 5′-CMP or 5′-TMP afforded only the thermodynamically stable adduct $[(\eta^6\text{-biphenyl})Ru(en)(N7\text{-GMP})]$.[30] Formation of H bonds between en-NH_2 groups of the ruthenium complex and C6O of guanine was found to enhance this selective coordination.[23,30] Such high selectivity of Ru to guanine has also been observed for reactions of the $(arene)Ru^{II}(en)$ complexes with oligonucleotides[31,32,34,37] and natural DNA[35,36] and is not affected by the presence of excess cytochrome *c*, L-histidine, or glutathione,[37,38] which may account for the low toxic side effects of such complexes compared with cisplatin.[22]

Chart 1. Ruthenium Arene Complex $[(\eta^6\text{-Biphenyl})Ru(en)Cl][PF_6]$ ($\mathbf{1}[PF_6]$) and Oligodeoxynucleotides (ODNs, I−X)[a]

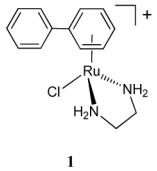

1

I: 5′-CTCTCT**T**$_7$**G**$_8$TC**T**$_{11}$TCTC-3′
II: 5′-CTCTC**T**$_6$C**G**$_8$AC**T**$_{11}$TCTC-3′
III: 5′-CTCTC**T**$_6$A**G**$_8$TC**T**$_{11}$TCTC-3′
IV: 5′-CTCTCT**T**$_7$**G**$_8$AC**T**$_{11}$TCTC-3′
V: 5′-C**T**$_2$ACCAC-3′
VI: 5′-CA**T**$_3$CCAC-3′
VII: 5′-CAC**T**$_4$CAC-3′
VIII: 5′-CACC**T**$_5$AC-3′
IX: 5′-CACCA**T**$_6$C-3′
X: 5′-AGGGTTAG**G**$_9$**G**$_{10}$TTA**G**$_{14}$**G**$_{15}$**GT**$_{17}$**T**$_{18}$A**G**$_{20}$GG-3′

[a]Potential binding sites for complex **1** are shown in red and bold.

However, using a combination of ladder-sequencing and top-down mass spectrometric approaches, we recently demonstrated that in the early stages (<2 h) of reactions of complex **1** with a series of 15-mer single-stranded oligodeoxynucleotides (ODNs, **I**−**IV**, Chart 1), the T_6, T_7, and T_{11} bases are ruthenation sites in addition to G_8.[39] This suggests that T bases are likely to be kinetically competitive binding sites for $\{(arene)Ru^{II}(en)Cl\}^+$ in single-stranded DNA or if there is T-base flipping out from the double helix.[40] Overhanging single-stranded 3′-ends are a feature of telomeres, and these regions containing, e.g., T2AG3, T2G4, or T4G4 repeats are often not only G rich but also T rich, of which the T bases are generally located on the loops and not H bonded when the single-stranded DNA forms G-quadruplexes.[41−45] Such unique DNA has been reported to be a promising potential target for cisplatin in cancer cells.[46] At low doses of cisplatin, the telomeres in cisplatin-treated HeLa cells are markedly shortened and degraded, which is sufficient to cause lethal damage in 61% of the cells. Interactions between cisplatin and human telomere G-quadruplex oligonucleotides $(AG_3(T_2AG_3)_3$ and $(T_2AG_3)_4)$ have also been explored,[47] where all four adenines in the loop of each sequence and 4 out of the 12 guanines are found to participate in the cross-links.

In order to further understand the roles of T binding in the action of the ruthenium arene anticancer complexes, in the present work we conducted a detailed kinetic study on reactions of complex **1** with single-stranded ODNs **I**−**IV** (Chart 1). Deoxydinucleotides 5′-TpG and 5′-GpT and a series of 7-mer single-thymine-containing ODNs (**V**−**IX**, Chart 1) were used to verify the kinetic binding preference of complex **1** for T bases in single-stranded ODNs. Also, such competition for binding to complex **1** between T and G in a human telomeric sequence which folds into a G-quadruplex has been investigated.

EXPERIMENTAL SECTION

Materials. $[(\eta^6\text{-bip})Ru(en)Cl][PF_6]$ ($\mathbf{1}[PF_6]$) (bip = biphenyl; en = ethylenediamine, Chart 1) was synthesized as described in the literature.[23,24] Triethylammonium acetate buffer (TEAA, 1 M) was purchased from AppliChem (Germany), acetonitrile (HPLC grade) from Tedia (USA), and D_2O (99.9%) from Cambridge Isotope Laboratories, Inc. (USA). The HPLC-purified oligodeoxynucleotides (**I**−**X**, Chart 1) were purchased from TaKaRa (Dalian, China), and the concentration of the ODNs was determined by UV spectroscopy at 260 nm. Bovine spleen phosphodiesterase (BSP) was bought from Sigma (USA) and dissolved in 10 mM TEAA buffer (pH 7) prior to use. Microcon YM-3 filter was purchased from Millipore (USA). Aqueous solutions were prepared using Milli-Q water (Milli-Q Reagent Water System). NMR experiments were performed in 10% D_2O/90% H_2O.

Sample Preparation. Stock solutions of complex **1** (5 or 10 mM), the dinucleotides (TpG and GpT, 10 mM), the 15-mer ODNs (**I**−**IV**, 1 mM), 7-mer ODNs (**V**−**IX**, 1 mM), and the 22-mer human telomeric ODN (**X**, 0.5 mM) were prepared by dissolving the respective complex and ODNs in deionized water and then diluting as required prior to use.

Kinetic study of the reaction of complex **1** with each 15-mer single-strand ODN was initiated by mixing a solution of 0.1 mM complex **1** and an equimolar amount of each ODN in 50 mM TEAA buffer (pH 7). The resulting solution was incubated at 310 K, and aliquots were withdrawn at various time intervals and then immediately injected for HPLC analysis. The same procedure was also applied for kinetic studies of reactions of complex **1** with the 7-mer ODNs.

For the NMR kinetic study of reaction between complex **1** and dinucleotide 5′-TpG or 5′-GpT, 10 mM complex **1** and 10 mM of either dinucleotide were mixed in NMR tubes containing 10% D_2O/90% H_2O of which the pH was adjusted to 7.3 by adding concentrated ammonia solution, and the ^1H NMR spectrum was recorded at 310 K over appropriate time intervals.

To anneal the single-stranded **X** into G-quadruplex (G4), the aqueous solution of ODN **X** was diluted to 100 μM by 50 mM TEAA buffer (pH 7) containing 50 mM $NaClO_4$. Then the resulting mixture in a quartz cuvette was heated in the temperature controller of a UV-2550 spectrophotometer (Shimadzu Corp., Japan) to 368 K over 0.5 h. The cuvette was kept at 368 K for 10 min, slowly cooled to the room temperature over 5 h, and then stored at 277 K overnight prior to CD spectroscopic analysis. The whole annealing process was monitored by UV spectroscopy with detection at 295 nm. The resulting G-quadruplex **X** (G4-**X**, 100 μM in 50 mM $NaClO_4$ and 50 mM TEAA, pH 7) was incubated with complex **1** at a molar ratio of Ru:X = 0.2:1 at 310 K, and an aliquot of the reaction mixture withdrawn at different time intervals was ultrafiltered by Microcon YM-3 to remove the unbound ruthenium complex at 277 K (low temperature was used to reduce dissociation of ODN-bound ruthenium) and then partially digested by BSP. Digestions were carried out at 310 K with 28 mU of BSP in 20 mM NH_4Ac buffer (pH 6.7) for 8 h prior to LC-MS analysis.

Kinetic Studies. Normalized peak areas (from UV detection at 260 nm) of HPLC fractions corresponding to unbound ODNs and ruthenated ODN adducts were used to calculate the concentrations of respective species in the reaction mixtures. The reaction pathway of complex **1** with strand **I** containing two nonequivalent (G and T) binding sites is depicted in Scheme 1, and the corresponding rate equations are as follows

$$d[\mathbf{I}]/dt = -k_1[\mathbf{1}][\mathbf{I}] - k_2[\mathbf{1}][\mathbf{I}] + k_{-1}[\mathbf{I} + \mathbf{1}'_G] + k_{-2}[\mathbf{I} + \mathbf{1}'_T] \quad (1)$$

dx.doi.org/10.1021/ic401606v | Inorg. Chem. 2013, 52, 11332−11342

Scheme 1. Reaction Pathways for Binding of Complex 1 to 15-mer Single-Stranded ODNs Containing Both G and T Bases[a]

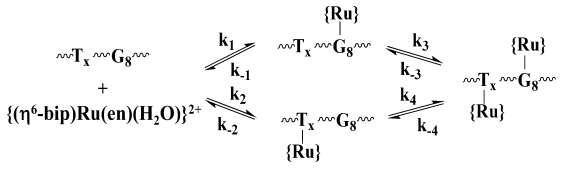

[a]The majority of **1** is present in the aquated form $[(\eta^6\text{-bip})Ru(en)(H_2O)]^{2+}$ in TEAA buffer (pH 7).[12,48] {Ru} = $\{(\eta^6\text{-bip})Ru(en)\}^{2+}$.

$$d[\mathbf{I} + \mathbf{1}'_G]/dt = k_1[\mathbf{1}][\mathbf{I}] - k_{-1}[\mathbf{I} + \mathbf{1}'_G] + k_{-3}[\mathbf{I} + \mathbf{1}'_2] - k_3[\mathbf{1}][\mathbf{I} + \mathbf{1}'_G] \quad (2)$$

$$d[\mathbf{I} + \mathbf{1}'_T]/dt = k_2[\mathbf{1}][\mathbf{I}] - k_{-2}[\mathbf{I} + \mathbf{1}'_T] + k_{-4}[\mathbf{I} + \mathbf{1}'_2] - k_4[\mathbf{1}][\mathbf{I} + \mathbf{1}'_T] \quad (3)$$

$$d[\mathbf{I} + \mathbf{1}'_2]/dt = k_3[\mathbf{1}][\mathbf{I} + \mathbf{1}'_G] + k_4[\mathbf{1}][\mathbf{I} + \mathbf{1}'_T] - k_{-3}[\mathbf{I} + \mathbf{1}'_2] - k_{-4}[\mathbf{I} + \mathbf{1}'_2] \quad (4)$$

where $[\mathbf{I}]$, $[\mathbf{1}]$, $[\mathbf{I} + \mathbf{1}'_G]$, $[\mathbf{I} + \mathbf{1}'_T]$, and $[\mathbf{I} + \mathbf{1}'_2]$ represent the instantaneous concentration of strand **I**, complex **1** (including aqua and chlorido species[48]), G-bound monoruthenated **I**, T-bound monoruthenated **I**, and diruthenated **I**, respectively. Rate constants were calculated by nonlinear computer fitting of the concentration/time data for the various species to eqs 1−4 using the program SCIENTIST.[49] The same calculation method was also applied to reactions of complex **1** with single-stranded **II**−**IV**. As there is more than one T binding site for complex **1** on these single strands and it is difficult to fully separate these different T-bound species by HPLC,[39] the relative HPLC peak areas corresponding to T-bound monoruthenated ODN adducts with different T-binding sites were summed to calculate the content of T-bound species. Such a nonlinear computer-fitting method was also applied to calculate the kinetic association and dissociation constants for interactions of complex **1** with 5′-TpG or 5′-GpT.

The rate constants for reactions of complex **1** with 7-mer monothymine-containing ODNs **V**−**IX**, in which the thymine base is the only binding site for complex **1**, were calculated by fitting the concentration/time data to the second-order reaction rate equation.

High-Performance Liquid Chromatography (HPLC). An Agilent 1200 series quaternary pump and a Rheodyne sample injector with a 20 μL loop, an Agilent 1200 series UV−vis DAD detector, and Chemstation data processing system were used. Mobile phases were water containing 20 mM TEAA (solvent A) and acetonitrile containing 20 mM TEAA (solvent B). Kinetic studies were carried out on a GLS Inertsil WP300 C18 reversed-phase column (2.1 × 50 mm, 5 μm, GL Sciences Inc.) with a flow rate of 0.2 mL min^{-1}. For separation of reaction mixtures of complex **1** with strands **I**−**IV**, the gradient (B) was 7−10% from 0 to 3 min, 10−11% from 3 to 10 min, 11−15% from 10 to 14 min, 15−80% from 14 to 15 min, and then 80−7% from 15 to 19 min. For separation of reaction mixtures of complex **1** with strands **V**−**IX**, the gradient (B) was 5% from 0 to 3 min, 5−30% from 3 to 15 min, 30−80% from 15 to 16 min and then keeping at 80% for 4 min, and finally resetting to 5% at 21 min.

Separation of the enzymatic digests of the ruthenated G4-**X** by complex **1** was carried out on a Varian Pursuit XRs C-18 reversed-phase column (2.0 × 100 mm, 3 μm, Varian, Inc.) with a flow rate of 0.2 mL min^{-1}, and the eluent was infused to the mass spectrometer (Micromass Q-TOF, Waters) with a splitting ratio of 1/2 for MS analysis. Gradient elution was achieved as follows (solvent B): 1% within 0−5 min, 1−20% over 5−30 min, 20−80% within 30−32 min, 80% over 32−37 min, resetting to 1% at 39 min.

Electrospray Ionization Mass Spectroscopy (ESI-MS). Negative-ion ESI mass spectra were obtained with a Micromass Q-TOF Ultima Global (Waters) equipped with a Masslynx (version 4.0) data processing system for analysis and postprocessing. The spray voltage and cone voltage were 3.3 kV and 35 V, respectively. The desolvation temperature was 413 K, and the source temperature was 358 K. Nitrogen was used as both cone gas and desolvation gas with a flow rate of 50 and 500 L/h, respectively. The collision energy was set up to 10 V. Spectra were acquired in the range of 200−2000 m/z. The mass accuracy of all measurements was within 0.01 m/z unit, and all m/z data are the mass-to-charge ratios of the most abundant isotopomer for the observed ions.

NMR Spectroscopy. ^{1}H NMR spectra were acquired on a Bruker Avance 600 (^{1}H = 600 MHz) NMR spectrometer using a BBI probe and equipped with z-field gradients. ^{1}H NMR spectra were typically acquired with 64 transients into 32 K data points over a spectral width of 18.0 kHz. Water suppression was achieved by presaturation with a relaxation delay of 2.0 s. All data processing was carried out using MestReNova 6.1.0 (Mestrelab Research S. L.). ^{1}H NMR chemical shifts were internally referenced to the residual water signal of D_2O (4.79 ppm).

Circular Dichroism (CD) Spectroscopy. Circular dichroism spectra were recorded at room temperature on a Jasco J-815 spectropolarimeter in the range 220−340 nm in 0.5 nm increments with an averaging time of 1 s and a scanning speed of 100 nm min^{-1}. The cell path length was 1 cm. Each spectrum was the average of five scans and corrected by blank buffer solution.

Thermal-Melting Assay. The melting temperature (T_m) of the G-quadruplex oligonucleotide **X** (G4-**X**) was measured using a UV-2550 spectrophotometer with a temperature controller (Shimadzu Corp., Japan). The G4-**X** oligonucleotides were incubated with various concentrations of complex **1** at 310 K for 24 h and diluted to give a final concentration of 20 μM (G4-**X**). Spectra of the reaction mixtures were then monitored at 295 nm over the range of temperature from 283 to 363 K with an increasing rate of 0.2 K min^{-1}, and T_m values were calculated by computer fitting of the absorbance/temperature data with Sigmoidal function.

RESULTS

Kinetics of Reactions of Complex 1 with Single-G-Containing Oligonucleotides. First, reaction of complex **1** with 1 mol equiv of each 15-mer ODN (**I**−**IV**, Chart 1) in TEAA buffer (pH 7) at 310 K was investigated by HPLC and LC-MS. We previously demonstrated that there are three potential binding sites for complex **1** on the studied ODNs (T_7, T_{11}, and G_8 on **I** and **IV**; T_6, T_{11}, and G_8 on **II** and **III**),[39] However, LC-MS analysis revealed that monoruthenated adducts are the predominant products formed by reactions of **1** with each ODN, accompanied by formation of a small amount of diruthenated adducts (Figure S1, Supporting Information).

Due to similar HPLC retention times, the T-bound monoruthenated adducts (labeled as c1 in Figure 1A and Figure S1A, Supporting Information) could not be fully separated. In particular, although tandem mass spectrometry (MS/MS) analysis indicated that both T_7 and T_{11} in **I** could be ruthenated by **1** to give rise to two monoruthenated ODN adducts,[39] there is only a singlet HPLC peak (c1 in Figure 1A) corresponding to the T-bound adducts. To simplify the kinetic study, the HPLC peak areas of T-bound monoruthenated adducts arising from each reaction was summed together as one single T-bound adduct. Thus, a pseudodivalent binding reaction pathway for complex **1** with each of the ODNs is proposed as shown in Scheme 1. The concentrations of the G- and T-bound species were calculated on the basis of the respective normalized HPLC peak areas detected at 260 nm,[50] and then the time-course data were computer fitted to the appropriate differential rate equations (Figure 1B and Figures

dx.doi.org/10.1021/ic401606v | Inorg. Chem. 2013, 52, 11332−11342

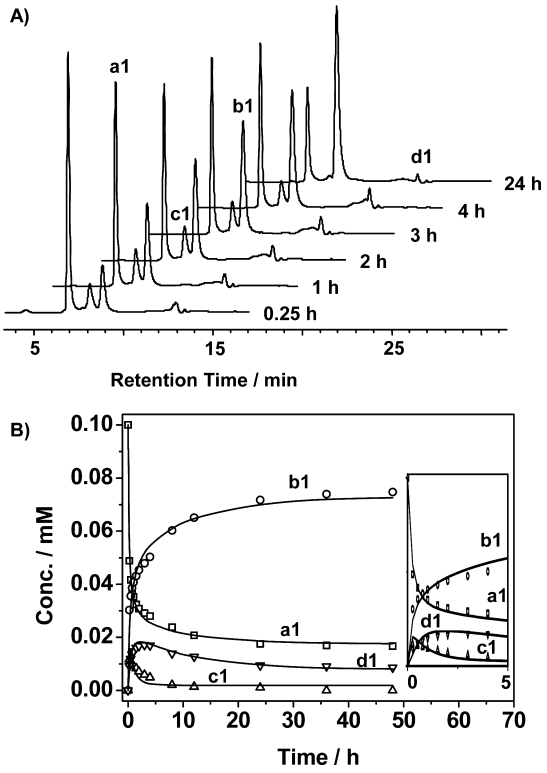

Figure 1. (A) HPLC time course for reaction of complex **1** with strand **I** ([**1**]/[**I**] = 1.0) in 50 mM TEAA (pH 7, 310 K). Peak assignments: a1, **I**; b1, G-bound monoruthenated **I**; c1, T-bound monoruthenated **I**; d1, diruthenated **I**. Mass spectra for the HPLC fractions are shown in Figure S1B, Supporting Information. (B) Experimental (points) and computer-fitted (lines) kinetic curves for reaction of complex **1** with **I**. (Inset) Enlarged curves between 0 and 5 h.

S2–S4, Supporting Information), giving the rate constants listed in Table 1.

Calculated rate constants (Table 1) indicate that the initial ruthenation (k_2 = 6.68 ± 0.50 M^{-1} s^{-1}) at either T_7 or T_{11} in strand **I** by **1** is competitive with ruthenation at G_8 (k_1 = 5.45 ± 0.15 M^{-1} s^{-1}). However, with an increase in time, the T-bound monoruthenated adducts (c1 in Figure 1A) converted to diruthenated adduct (d1) via the second step of fast ruthenation at G_8 (k_4 = 9.67 ± 0.64 M^{-1} s^{-1}) and then partially to the G-bound monoruthenated product (b1) via dissociation of the T-bound (bip)Ru^{II}(en) fragment from the diruthenated adduct, reflected in the decrease in concentration of the diruthenated adduct accompanied by an increase in content of G_8-bound monoruthenated adduct (Figure 1B). The T-bound species became undetectable after 36 h reaction when formation of both G-bound monoruthenated and diruthenated adducts reached equilibrium. Notably, ruthenation by **1** at T_7 or T_{11} in **I** appears to be positively cooperative to ruthenation at G_8. The second step binding of **1** to G_8 (k_4) in T-bound monoruthenated **I** (T_i-Ru-**I**) (i = 7 or 11[39]) is ca. 1.8-fold faster than the first step binding of **1** to G_8 (k_1) in **I**. In contrast, G_8 binding of **1** largely retards further ruthenation of the G_8-Ru-**I** at T_7 or T_{11}. The rate constant for ruthenation of T bases on G_8-Ru-**I** is about 270-fold smaller than that for the first step binding at T bases in **I** (Table 1). The site binding constant of **1** to T ($K = k_2/k_{-2}$ = (1.37 ± 0.42) × 10^4 M^{-1}) in **I** is nearly 30-fold smaller than that to G_8 ($K = k_1/k_{-1}$ = (4.22 ± 0.96) × 10^5 M^{-1}) in **I**, also providing evidence that the T-bound monoruthenated adducts are not thermodynamically favored. However, a small amount of T_iG_8-bound diruthenated adduct (peak d1 in Figure 1B) was still detectable, accounting for ca. 10% of the total amount of **I** in the 36 h reaction mixture of complex **1** with **I**.

The base changes on both sides of G_8 in strand **II** (Chart 1) appear to strengthen the ability of the T bases to compete with G_8 for binding to **1**, but the synergetic effect of T binding on the second step of G_8-ruthenation of the T_i-Ru-**II** (i = 6 or 11[39]) adduct diminished, as seen by the value change from k_1 to k_4 (k_4/k_1 = 1.0, Table 1). Such a decrease in positive cooperativity of T_i binding for G_8 binding was also observed for reaction of **1** with strand **III** or **IV**, although the sequence change occurred only on either the 5′- or the 3′-side of G_8 compared to **I**. Only a small increase from k_1 to k_4 (k_4/k_1 = 1.4 for both **III** and **IV**) was observed for both strands (**III** and **IV**).

Kinetics of Reactions of Complex 1 with GpT/TpG. To further verify the kinetic competition between thymine and guanine for binding to complex **1** and formation of the diruthenated oligonucleotide adducts, the binding reactions of complex **1** with deoxydinucleotides 5′-TpG and 5′-GpT were studied kinetically by ^{1}H NMR spectroscopy. NMR time courses for reaction of complex **1** with TpG and GpT are shown in Figure 2A and 2B, respectively. Assignments of different species are based on the ^{1}H chemical shift of T-CH_3.[30] The results indicate that three products are formed in each reaction, namely, G-bound and T-bound monoruthenated dinucleotides and T,G-bound diruthenated adducts (labeled as b, c, and d, respectively, in Figure 2). The pH of the reaction mixtures decreased from 7.3 (initial) to 6.7 and 6.4 for TpG and GpT, respectively, compatible with N3 coordination to Ru and concomitant N3H deprotonation.[30] These reactions are consistent with the binding pathways shown in Scheme 1. On

Table 1. Rate Constants for Reactions of Complex 1 With Single Strands I–IV at 310 K[a]

	k_1/M^{-1} s^{-1}	k_2/M^{-1} s^{-1}	k_3/M^{-1} s^{-1}	k_4/M^{-1} s^{-1}
1 + **I**	5.45 ± 0.15	6.68 ± 0.50	0.0240 ± 0.0223	9.67 ± 0.64
1 + **II**	3.18 ± 0.40	3.73 ± 0.14	0.899 ± 0.420	3.21 ± 0.11
1 + **III**	5.91 ± 0.08	3.71 ± 0.13	0.348 ± 0.016	8.24 ± 0.25
1 + **IV**	3.00 ± 0.10	4.15 ± 0.26	0.168 ± 0.004	4.26 ± 0.28
	k_{-1}/s^{-1}	k_{-2}/s^{-1}	k_{-3}/s^{-1}	k_{-4}/s^{-1}
1 + **I**	(1.29 ± 0.21) × 10^{-5}	(4.86 ± 0.85) × 10^{-4}	(2.12 ± 0.22) × 10^{-5}	0
1 + **II**	(7.21 ± 0.27) × 10^{-6}	(1.27 ± 0.03) × 10^{-4}	(4.78 ± 0.82) × 10^{-5}	0
1 + **III**	(4.22 ± 0.54) × 10^{-6}	(1.44 ± 0.06) × 10^{-4}	(1.18 ± 0.04) × 10^{-5}	0
1 + **IV**	(7.35 ± 0.13) × 10^{-6}	(1.16 ± 0.09) × 10^{-4}	(1.85 ± 0.10) × 10^{-5}	0

[a]Reaction pathway is shown in Scheme 1.

dx.doi.org/10.1021/ic401606v | Inorg. Chem. 2013, 52, 11332–11342

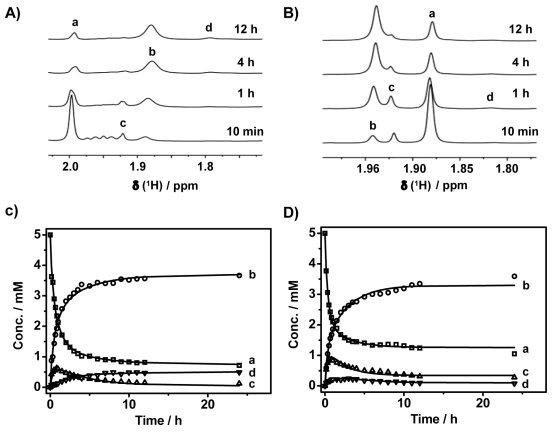

Figure 2. (A and B) ^{1}H NMR time course for reaction of 1 with 5′-TpG (A) or 5′-GpT (B) (1:1, 5 mM) at 310 K. Peak assignments: a, free TpG or GpT; b, G-bound monoruthenated TpG or GpT; c, T-bound monoruthenated TpG or GpT; d, diruthenated TpG or GpT. (C and D) Experimental (points) and computer-fitted (lines) kinetic curves for reaction of complex **1** with 5′-TpG (C) or 5′-GpT (D).

the basis of the integrated intensity of the ^{1}H NMR signals of T-CH_3 for different species, time-course data (Figure 2C and 2D) were computer-fitted to the appropriate differential rate equations, giving the rate constants listed in Table 2.

The results indicate that the competition between T and G for binding to **1** is also observed for these dinucleotides. The rate constant for binding of **1** to the T in GpT ($(4.95 \pm 0.16) \times 10^{-2}$ $M^{-1}s^{-1}$) is only slightly smaller than that for binding of **1** to the G ($(5.98 \pm 0.06) \times 10^{-2}$ $M^{-1}s^{-1}$) in GpT. Compared with the T in GpT, however, the competitive ability of the T in TpG decreases, the rate constant of **1** to the T in TpG ($(2.04 \pm 0.04) \times 10^{-2}$ $M^{-1}s^{-1}$) is only one-third of that for the binding of **1** to the G ($(6.02 \pm 0.10) \times 10^{-2}$ $M^{-1}s^{-1}$). Unlike the binding of complex **1** to the 15-mer single-stranded ODN **I**, no synergetic effect of T binding on the second step of ruthenation at G in the T-bound TpG and GpT adducts was observed (k_4/k_1 = 0.6 for TpG and 0.5 for GpT). G binding appeared to prevent the second step of ruthenation at T in the G-bound TpG and GpT adducts, reflected in $k_3 = 0$. Similar to the T-bound monoruthenated ODNs **I**–**IV**, the T-bound ruthenated TpG adduct was not thermodynamically stable and eventually converted to the T,G-bound diruthenated adduct, which accounted for ca. 10% of the total amount of TpG in the 24 h reaction mixture of complex **1** with TpG, while the G,T-bound diruthenated GpT adduct eventually converted to the G-bound monoruthenated species with a half-life of 1.8 h and almost disappeared after 24 h reaction. It is notable that despite the transformation of the T-bound monoruthenated GpT slowly to the G,T-bound diruthenated adduct, it was still detectable and accounted for ca. 6% of the total amount of GpT in the 24 h reaction mixture. Additionally, the site binding constant of complex **1** for 3′-G in TpG ($K = k_1/k_{-1} = (1.31 \pm 0.03) \times 10^4$ M^{-1}) is ca. 6-fold larger than that to 5′-G in GpT ($(2.19 \pm 0.11) \times 10^3$ M^{-1}), indicating that complex **1** preferentially binds to a 3′-G over a 5′-G.

Kinetics of Reactions of Complex 1 with Single-T-Containing Oligonucleotides. It is notable that the middle thymine bases, such as T_7 and T_{11} in strands **I** and **IV** and T_6 and T_{11} in strands **II** and **III**, are more kinetically favored than the terminal thymines (T_2 and T_{14}) for binding to complex **1**. To further verify the kinetic binding preference of complex **1** to thymine bases in single-stranded ODNs, we studied the kinetics of binding of complex **1** to a series of 7-mer oligonucleotides which contain a single thymine base located at different position of the sequences (**V**–**IX**, Chart 1). HPLC assays demonstrated that only one product formed by reaction of **1** with each of the 7-mer ODNs (Figure 3A), and MS confirmed

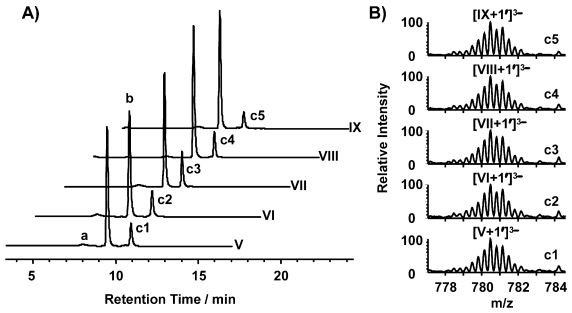

Figure 3. (A) Chromatograms with UV detection at 260 nm for reaction mixtures of complex **1** with equimolar amounts of ODNs **V**–**IX** (in 50 mM TEAA, pH 7) incubated at 310 K for 24 h. Peak assignments: a, aqua product of complex **1**; b, unbound ODNs; c1–c5, T-bound monoruthenated ODNs. (B) Mass spectra of the HPLC fractions c1–c5 in A.

it as a monoruthenated ODN adduct (Figure 3B). Taking the relatively higher affinity of **1** for T compared to A and C into account, the binding site of **1** in ODNs **V**–**IX** is most likely the single T in each sequence (Chart 1). HPLC time courses for reactions of complex **1** with the five 7-mer ODNs are shown in Figure 4A and Figures S5–S8, Supporting Information, and kinetic constants were then calculated by fitting the kinetic data to the rate equation of a single-site binding reaction (Figure 4B) and are listed in Table 3. The results indicate that T_4 in **VII** has the largest association rate constant ($k_a = 0.446 \pm 0.018$ M^{-1} s^{-1}) for binding to **1** than the T bases in other 7-mer ODNs and that the rate constant ($k_d = (5.33 \pm 0.30) \times 10^{-5}$ s^{-1}) of the corresponding dissociation is also large. As a consequence, the site binding constant for binding of **1** to T_4 in

Table 2. Rate Constants for Reactions of Complex 1 With Dinucleotides 5′-TpG and 5′-GpT at 310 K[a]

	k_1/M^{-1} s^{-1}	k_2/M^{-1} s^{-1}	k_3/M^{-1} s^{-1}	k_4/M^{-1} s^{-1}
	1 to G	**1** to T	**1** to G, then T	**1** to T, then G
1 + TpG	$(6.02 \pm 0.10) \times 10^{-2}$	$(2.04 \pm 0.04) \times 10^{-2}$	0	$(3.86 \pm 0.02) \times 10^{-2}$
1 + GpT	$(5.98 \pm 0.06) \times 10^{-2}$	$(4.95 \pm 0.16) \times 10^{-2}$	0	$(2.84 \pm 0.16) \times 10^{-2}$
	k_{-1}/s^{-1}	k_{-2}/s^{-1}	k_{-3}/s^{-1}	k_{-4}/s^{-1}
1 + TpG	$(3.07 \pm 0.30) \times 10^{-6}$	$(6.24 \pm 0.21) \times 10^{-5}$	0	0
1 + GpT	$(2.90 \pm 0.07) \times 10^{-5}$	$(1.72 \pm 0.06) \times 10^{-4}$	$(1.07 \pm 0.06) \times 10^{-4}$	0

[a]Reaction pathways are similar to that of complex **1** with 15-mer ODNs shown in Scheme 1.

dx.doi.org/10.1021/ic401606v | Inorg. Chem. 2013, 52, 11332–11342

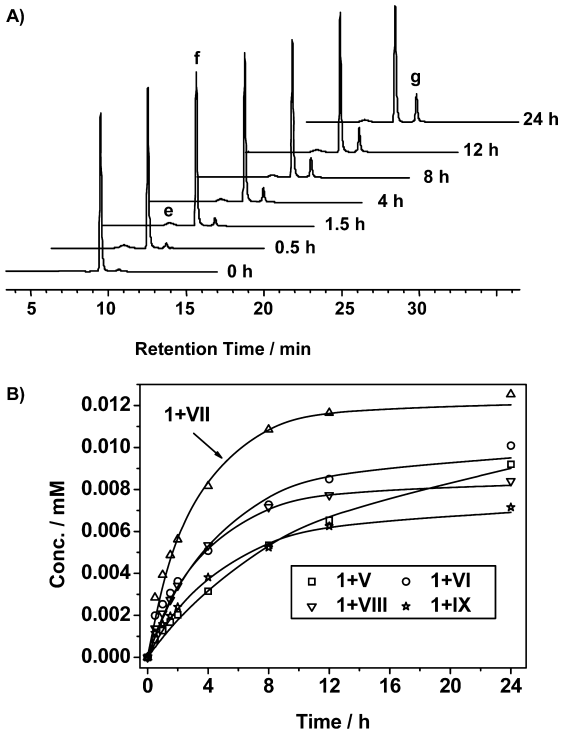

Figure 4. (A) HPLC time course for reaction of complex **1** with 1 mol equiv of strand **VII** in 50 mM TEAA (pH 7) at 310 K. Peak assignments: a, aqua adduct of **1**; b, **VII** and c, T-bound monoruthenated **VII**. (B) Experimental (points) and computer-fitted (lines) kinetic curves for reaction of complex **1** with ODNs **V**–**IX**.

Table 3. Rate Constants (k) and Site Binding Constants (K) for Reactions of Complex 1 with 7-mer Single-Stranded ODNs V–IX (Chart 1) at 310 K

	k_a[a]/M^{-1} s^{-1}	k_d[a]/s^{-1}	$K(k_a/k_d)$/M^{-1}
1 + **V**	0.110 ± 0.004	(1.77 ± 0.13) × 10^{-5}	(6.23 ± 0.72) × 10^3
1 + **VI**	0.232 ± 0.014	(3.98 ± 0.35) × 10^{-5}	(5.84 ± 0.94) × 10^3
1 + **VII**	0.446 ± 0.018	(5.33 ± 0.30) × 10^{-5}	(8.36 ± 0.84) × 10^3
1 + **VIII**	0.248 ± 0.005	(5.27 ± 0.14) × 10^{-5}	(4.70 ± 0.22) × 10^3
1 + **IX**	0.158 ± 0.006	(4.21 ± 0.23) × 10^{-5}	(3.76 ± 0.37) × 10^3

[a] k_a and k_d represent the rate constants for association and dissociation, respectively

VII ($K = k_a/k_d = (8.36 \pm 0.84) \times 10^3$ M^{-1}) is the largest one. Comparing the site binding constants of complex **1** for the T bases in the five 7-mer ODNs, we found that the binding affinity of complex **1** for the T bases decreases in the order of T_4 in **VII** > T_3 in **VI** ≈ T_2 in **V** > T_5 in **VIII** > T_6 in **IX**. These results indicate that complex **1** has higher affinity for the middle T than a terminal T in a sequence and preferentially binds to a 5′-side T rather than to a 3′-T in an oligonucleotide.

Competition of Thymines with Guanines in Human Telomeric G-Quadruplex DNA for Binding to Complex 1. The 22-mer oligonucleotide **X** (Chart 1) is a 3′-end sequence of a human telomere[51,52] and often folds into an intramolecular G-quadruplex (G4) conformation, termed G4-**X**, where the G bases form the quartets via H bonding and the T bases are usually located in relatively flexible loops. The N3 of T bases is therefore likely to be accessible for ruthenium coordination. To explore the competition between T-N3 and G-N7 in G4 DNA for binding to ruthenium arene anticancer complexes, interactions between complex **1** and G4-**X** were investigated. First, the single-stranded ODN **X** was annealed in 50 mM $NaClO_4$ solution, and the CD spectrum showed that antiparallel G4-**X**[44,53] was formed (Figure 5A). CD analysis

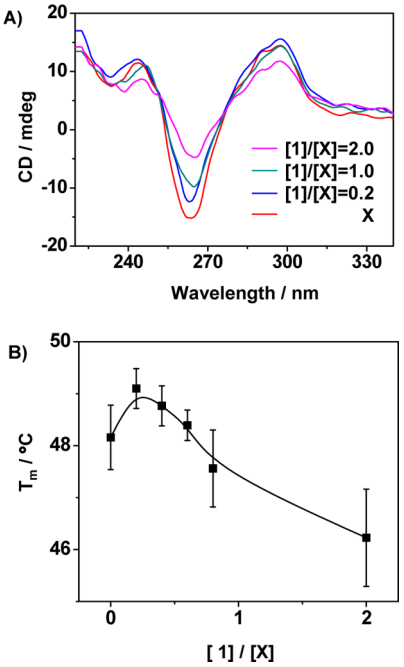

Figure 5. (A) CD spectra of G4-**X** (5 μM) and reaction mixtures of G4-**X** with various concentrations of complex **1** in 50 mM $NaClO_4$ at 310 K for 24 h. (B) Melting temperature (T_m) of the ruthenated G4-**X** (5 μM) formed by reaction of complex **1** in 50 mM $NaClO_4$ at 310 K for 24 h.

also indicated that high concentrations of complex **1** disrupted the antiparallel G4 conformation of strand **X**. Further study demonstrated that when the molar ratio of complex **1** to **X** was lower than 0.2, the melting temperature of G4-**X** increased slightly due to ruthenium coordination (Figure 5B), suggesting that complex **1** at low concentration stabilized the G4-**X** to some extent. However, when the molar ratio of complex **1** to **X** further increased, the melting temperature of G4-**X** decreased with increaseing concentration of complex **1** (Figure 5B). Therefore, a low reaction molar ratio of **1** to **X** (0.2) was applied to study the binding preference of complex **1** to G4-**X**.

The purified ruthenated G4-**X** formed by reaction of complex **1** with G4-**X** at 310 K for 24 h was analyzed by LC-ESI-MS following digestion by bovine spleen phosphodiesterase (BSP). The exonuclease BSP sequentially removes mononucleotides from the 5′-terminus of single-stranded ODNs, and ruthenation on oligonucleotides arrested the exonucleolytic hydrolysis at or before the binding sites (Figure 6A).[39] This afforded 10 ruthenated 3′-end fragments (F^*_i and F^*_{i+1}, Figure S9, Supporting Information, Table 4), for which the characteristic isotopic pattern (Figure S10, Supporting Information) resulting from incorporation of the isotope-rich ruthenium makes them distinguishable from metal-free ODN fragments.[39,54] There were five pairs of the ith and $(i + 1)$th ruthenated fragments, namely, F^*_9 and F^*_{10}, F^*_{13} and F^*_{14}, F^*_{14} and F^*_{15}, F^*_{17} and F^*_{18}, and F^*_{19} and F^*_{20}, detected by MS analysis of the BSP digest of the ruthenated G4-**X**. Considering the apparent discrimination of complex **1** between guanine and adenine,[30] the ruthenation sites on F^*_{13} and F^*_{14} and F^*_{19} and F^*_{20} are

dx.doi.org/10.1021/ic401606v | Inorg. Chem. 2013, 52, 11332–11342

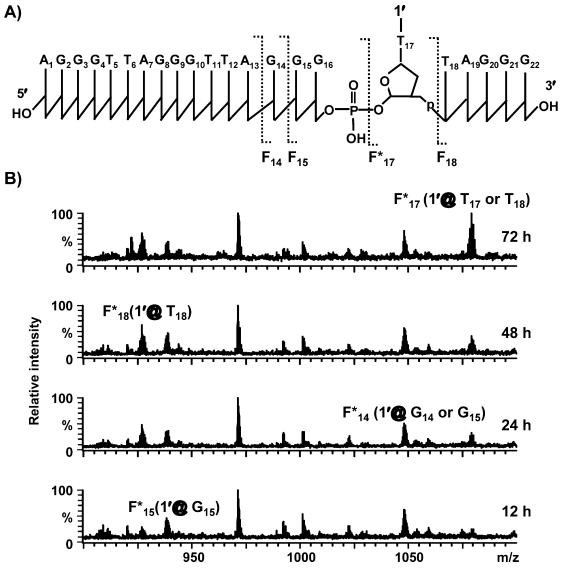

Figure 6. (A) Schematic representation of exonuclease (BSP) digestion of ODN **X** with ruthenium fragment $\{(\eta^6\text{-bip})\text{Ru(en)}\}^{2+}$ (**1′**) binding to T_{17} or T_{18}. F_i indicates the 3′-side fragment and F^*_i the respective monoruthenated fragment. (B) Mass spectra over the m/z range of 900−1100 for the BSP digest of the ruthenated G4-**X** produced by reaction of G4-**X** with complex **1** ([**X**]/[**1**] = 5) at 310 K for various times.

most likely G_{14} and G_{20}, respectively.[55] On the ruthenated fragment F^*_9, the binding site can be either G_9 or G_{10} and on F^*_{17} either T_{17} or T_{18}. Because there were no $(i-1)$th ruthenated fragments detected or corresponding ith ruthenated fragments F^*_{10}, F^*_{15}, and F^*_{18} (Figure S9, Supporting Information, Table 4), the ruthenation sites on these fragments are unambiguously assigned to G_{10}, G_{15}, and T_{18}, respectively.

On the basis of the MS signal intensity of the ruthenated fragments (Figure S9, Supporting Information), complex **1** appeared to bind preferentially to G_{14} and G_{20} of G4-**X** until 48 h. However, with increase in reaction time, the relative MS signal intensity of T_{17}- and/or T_{18}-bound ruthenated fragments markedly increased whereas the signal intensity of G_{14}- and G_{15}-ruthenated fragments did not change after 12 h reaction (Figure 6). These results suggest that thymines in this G4 ODN can compete with guanines for binding to complex **1**, forming thermodynamically stable adducts.

DISCUSSION

It is acknowledged that binding to DNA is essential for the cytotoxicity of the classical chemotherapeutic metallodrug cisplatin.[4−6] Although there is no direct correlation between the amount of ruthenated DNA formed inside cells and the cytotoxicity of the ruthenium arene complexes, maintenance of Ru on DNA strands is likely to cause persistent damage and affect DNA replication or transcription.[36] The amount of DNA-bound ruthenium detected in MCF-7 human breast cancer cells exposed to complex **1** or its analog $[(\eta^6\text{-}p\text{-cymene})\text{Ru(en)Cl}]^+$ is even larger than that of DNA-bound platinum detected in MCF-7 cells treated with the same concentration of cisplatin.[56] Therefore, exploration of the kinetics and thermodynamics of binding of ruthenium arene complexes to DNA is very important for further understanding of the mechanism of action of this class of organometallic anticancer complexes.

The class of ruthenium arene complexes $[(\eta^6\text{-arene})\text{Ru(en)Cl}]^+$ (arene = e.g., *p*-cymene, biphenyl, dihydroanthracene, or tetrahydroanthracene) has been previously shown to be non-cross-resistant to cisplatin toward human ovarian cancer cell line A2780 in vitro and in vivo.[22] This implies that the organometallic ruthenium complexes may exert anticancer activity involving a different mechanism from that of cisplatin. In other words, given that DNA is a potential target for ruthenium arene complexes,[35,36] they may attack DNA in a different way from cisplatin. In this regard, complex **1** and its analogs have been shown to be more discriminatory between G and A bases than cisplatin, which binds strongly to both guanine and adenine, forming intra- and interstranded cross-linking DNA adducts.[4] The affinity of the ruthenium arene complexes to mononucleosides decreases in the order G > T ≫ C > A.[23,30] However, reacting with native DNA in cell-free media[35] and single/double-stranded oligonucleotides in aqueous solutions,[32] complex **1** appeared to bind to guanine bases only. One possible explanation is the amount of thymine-bound DNA adducts may be too low to be detected by chemical mapping[36] or NMR spectroscopy[32] in the presence of highly abundant guanine-bound adducts. Another possible reason for the lack of observed thymine binding may be that thymine-bound ruthenated DNA adducts are not thermodynamically stable, so dissociate, and subsequently, Ru migrates to the thermodynamically favored guanine sites after longer reaction times.

The kinetic studies reported here demonstrate that the thymine bases (T_7 or T_{11} in single-stranded ODNs **I** and **IV**, T_6 or T_{11} in **II** and **III**) are indeed kinetically competitive with the

Table 4. Ruthenated Fragments Observed for the BSP Digest of Ruthenated G4-X by LC-ESI-MS[a]

fragment sequence	charge	observed (calcd) m/z[b]	ruthenation site
F^*_9: $G_9GTTAGGGTTAGGG_{22}$ + **1′**[c]	−3	1574.294(1574.258)	G_9 or G_{10}
F^*_{10}: $G_{10}TTAGGGTTAGGG_{22}$ + **1′**	−3	1465.254(1465.242)	G_{10}
F^*_{13}: $A_{13}GGGTTAGGG_{22}$ + **1′**	−3	1152.509(1152.531)	G_{14}
F^*_{14}: $G_{14}GGTTAGGG_{22}$ + **1′**	−3	1048.155(1048.172)	G_{14} or G_{15}
F^*_{15}: $G_{15}GTTAGGG_{22}$ + **1′**	−2	1408.247(1408.242)	G_{15}
F^*_{15}: $G_{15}GTTAGGG_{22}$ + **1′**	−3	938.484(938.492)	G_{15}
F^*_{17}: $T_{17}TAGGG_{22}$ + **1′**	−2	1079.186(1079.188)	T_{17} or T_{18}
F^*_{18}: $T_{18}AGGG_{22}$ + **1′**	−2	927.153(927.164)	T_{18}
F^*_{19}: $A_{19}GGG_{22}$ + **1′**	−2	775.145(775.141)	G_{20}
F^*_{20}: $G_{20}GG_{22}$ + **1′**	−2	618.606(618.612)	G_{20}

[a]Corresponding mass spectra are shown in Figures S9 and S10, Supporting Information. [b]Mass-to-charge ratio of the most abundant isotopmer. [c]**1′** = $\{(\eta^6\text{-bip})\text{Ru(en)}\}^{2+}$.

dx.doi.org/10.1021/ic401606v | *Inorg. Chem.* 2013, 52, 11332−11342

central guanine base G_8 for binding to complex **1**. However, the T-bound monoruthenated ODN adducts eventually convert to either diruthenated products via a second step of ruthenation at the G site or to G-bound monoruthenated species via dissociation of the T-bound ruthenium fragments. The T-bound monoruthenated adducts were almost undetectable after 36 h reaction when formation of G-bound monoruthenated and G,T-bound diruthenated adducts had reached equilibrium (Figures 1B and S2−S4). In the equilibrated reaction mixture of strand **I** with 1 mol equiv of complex **1**, the G-bound monoruthenated and G,T-bound diruthenated adduct accounted for ca. 75% and 9% of the total amount of **I**, respectively (Figure 1B).

The thermodynamic stability of guanine-bound adducts of complex **1** has been previously demonstrated by monitoring the competitive reaction of complex **1** with equivalent mononucleotides 5′-GMP, 5′-AMP, 5′-CMP, and 5′-TMP. This gave rise to the G-bound complex $[(\eta^6\text{-bip})\text{Ru(en)(N7-GMP)}]$ as the final thermodynamically stable product.[30] Such selectivity for guanine is strongly aided by H bonding between the en-NH_2 groups of the ruthenium complex and C6O of guanine[30] and hydrophobic interactions, in particular, intercalation of the biphenyl ligand between the neighboring bases.[31−33] The N3 of thymine base has a high pK_a (9.8); protonation is highly competitive with ruthenium binding to T-N3 at neutral pH.[30] Such competition is most likely responsible for the lower affinity of the ruthenium arene complexes to T compared to G and for the high rate of dissociation of T-bound ruthenium fragments, though the initial noncovalent electrostatic attraction between cationic Ru complex and anionic phosphate backbone and the H bonding between en-NH_2 groups of complex **1** and the C2O and/or C4O of thymine may also favor binding of **1** to T.[30] Formation of H bonds between cyclen NH of anti-HIV agent Zn(II)-[12]aneN4 and the C2 and C4 carbonyl oxygens of T or U has been shown to strengthen the highly selective coordination of zinc(II) complexes with cyclen ligands to thymidine.[57,58] Cisplatin has also been found to bind to thymine N3 sites on reaction with single-stranded dT_{20} oligonucleotide, which contains no guanine, at 298 K at pH 3.5 ± 0.5 as revealed by 2D $[^1H,^{15}N]$ HMQC NMR spectroscopy.[59] Computational results indicate that Pt^{II} initially binds to O4 and/or O2 of the canonical thymine tautomer and then migrates to N3 after its deprotonation.[60] The N3,O4-cross-linked adduct between cisplatin and thymine[61] was initially formed during the first two days and subsequently rearranges to N3,N3-cross-links in a very slow reaction.[59] For the monofunctional ruthenium complex **1**, similar recognition of Ru by oxygen in the reaction with thymine may also be involved. Ruthenium coordination to phosphate oxygen has been observed in the interactions of complex **1** with 5′-NMP (N = G, T, C, or A) nucleotides where the first stage was Ru−O(phosphate) binding, and such adducts were still present at equilibrium for T, C, and A nucleotides.[30] For oligonucleotides, however, steric hindrance and highly charged phosphate groups might make Ru binding to T-O2 or -O4 less significant.

Interestingly, ruthenation of T_7 or T_{11} in **I** exhibits markedly positive cooperativity with the second step of ruthenation at G_8, for which the rate constant is 1.8-fold larger than for the first step of binding of **1** to G_8 in **I** (Table 1). However, a sequence change to either the 5′- or the 3′-side of the central guanine (G_8) appears to weaken this synergetic effect of T binding on the second step of ruthenation at G_8. For polyanionic DNA and the monofunctional cationic complex $[(\eta^6\text{-arene})\text{Ru(en)}(H_2O)]^{2+}$, which is the reactive species of complex **1** produced by hydrolysis in aqueous solution,[48] electrostatic interactions and H bonding are involved in the initial recognition of Ru complexes prior to coordination to DNA.[30] Such reversible noncovalent binding significantly affects the rate and site preference of DNA metalation during the kinetically controlled interactions of metal complexes and nucleic acids.[62] Variations in the neighboring bases of G_8 may cause a change in the microenvironment that in turn modulates metal coordination. Collectively, these results imply that the oligonucleotide sequences can play an important role not only in site preference but also in the kinetic relationship between the binding of **1** to G and T bases in oligonucleotides. The preferential binding sites on DNA of Pt-based anticancer complexes, e.g., cisplatin and oxaliplatin, were also found to be highly dependent on the bases flanking the G sites.[63,64] The rate constant for diaqua cisplatin *cis*-$[Pt(NH_3)(H_2O)_2]^{2+}$ binding to the middle G in −XGY− sequences decreased in the order TGG > GGT > TGA ≈ AGT > GGC ≈ TGT > TGC. The very low reactivity of TGC sequence was thought to be a combined effect of the steric bulk of the flanking pyrimidines and of low negative molecular electrostatic potential (MEP). The similar reactivity of TGA and AGT toward the doubly charged cation *cis*-$[Pt(NH_3)(H_2O)_2]^{2+}$ was attributed to the compensation between the higher negative MEP of AGT and a higher accessibility of TGA.[63] Similarly, $[Pt(NH_3)_2(H_2O)_2]^{2+}$ displays no preference for the 3′- or 5′-guanine of a TpGpGpT sequence of a hairpin duplex oligonucleotide[65] and a single-stranded oligonucleotide.[66] However, when the sequence is TpGpGpC, the 5′-guanine is preferred by a factor of 2 in the case of a single-stranded oligonucleotide and by a factor of 12 in the case of duplex oligonucleotide.[67] Thus, DNA structure has a primary influence on selective binding of cationic metal-based anticancer complexes to DNA.[68−71] The widely different environment around the binding sites (e.g., guanine bases) in DNA may lead to a distinct selection of ruthenation sites by affecting the MEP at the site of the N7 lone pair and exerting different steric hindrances for complexes to approach guanine N7, consequently causing specific damage to DNA.

The competition between T and G for binding to complex **1** and formation of diruthenated adducts were also observed in reactions of complex **1** with dinucleotides TpG and GpT, which are the smallest components of oligonucleotides. Notably, diruthenated TpG adduct is thermodynamically stable, as evidenced by $k_{-3} = k_{-4} = 0$ (Table 2), and accounts for ca. 10% of the total amount of TpG in the 24 h reaction mixture of complex **1** with TpG. However, the diruthenated GpT adduct is not thermodynamically favored, transforming slowly to G-bound species through dissociation of T-bound ruthenium fragment with a half-life of 1.8 h, and almost disappeared after 24 h reaction. This suggests that the diruthenated TpG adduct is more stable than the diruthenated GpT adduct. It is worth pointing out that although the diruthenated GpT adduct is less stable than diruthenated TpG, the T-bound monoruthenated GpT species appears to be more thermodynamically favored than the T-bound monoruthenated TpG, accounting for ca. 6% of the total amount of GpT in the 24 h reaction mixture of complex **1** with GpT (Figure 2D), while the comparable value of the T-bound monoruthenated TpG is 2.6% (Figure 2C).

Using a series of 7-mer single-stranded ODNs (**V**−**IX**), which contain no G base but a single T base located at a different position of the strands, our further kinetic studies

dx.doi.org/10.1021/ic401606v | *Inorg. Chem.* 2013, 52, 11332−11342

showed that complex **1** preferentially binds to the central T base in single-stranded ODNs. The rate constant (k_a = 0.446 ± 0.018) for the binding of Ru to the central T in **VII** is the largest in the series of 7-mer single T-containing ODNs (Table 3), but it decreased gradually when T shifts to either the 5′- (in **V** and **VI**) or the 3′-terminus (in **VIII** and **IX**). The site binding constant of complex **1** for the central thymine T_4 in **VII** (Chart 1) is 2.2-fold higher than that for T_6 of **IX** near the 3′-terminus and 1.3-fold higher than that for T_2 of **V** near to the 5′-terminus. Collectively, these results suggest that complex **1** preferentially binds to middle T bases compared to T bases near the terminus of ODNs. Such preferential binding to the central G base of ODNs has also been observed for other Ru and Pt complexes and is significantly modulated by the initially noncovalent association, including hydrogen bonding, hydrophobic and electrostatic interactions between cationic metal complexes, and polyanionic nucleic acids.[54,62,72−77] For example, platination of guanine in the single-stranded ODNs $d(T_nGT_{16-n})$ is kinetically favored for *cis*-$[PtCl(NH_3)(c\text{-}C_6H_{11}NH_2)(H_2O)]^+$ (c-$C_6H_{11}NH_2$ = cyclohexylamine) when the G-N7 site was positioned in the middle of the oligomers but decreases gradually as the guanine is moved toward either the 5′- or the 3′-terminus.[76] Our previous reports demonstrated that $[(\eta^6\text{-arene})Ru(en)(H_2O)]^{2+}$ (arene = *p*-cymene or biphenyl) also bind selectively to G_6 and G_{11} bases in the middle of a single-stranded oligonucleotide 5′-GAGAA-G_6ACAAG$_{11}$AGAG-3′.[54]

Our kinetic studies also show that the site binding constants of complex **1** for T_2 ($(6.23 \pm 0.72) \times 10^3$ M^{-1}) in **V** and T_3 ($(5.84 \pm 0.94) \times 10^3$ M^{-1}) in **VI** near to the 5′-termini are higher than those to T_5 ($(4.70 \pm 0.22) \times 10^3$ M^{-1}) in **VIII** and T_6 ($(3.76 \pm 0.37) \times 10^3$ M^{-1}) in **IX** near to the 3′-termini (Table 3). These suggest that complex **1** prefers coordination to the 5′-side T bases rather than to 3′-side T bases. Cisplatin has been also shown to bind preferentially to a 5′-A over a 3′-A adjacent to G in interactions with oligonucleotides, and binding of cisplatin to AG sequences is somewhat faster than to GA sequences.[7,8,78−80] For example, for reaction of *cis*-$[PtCl_2(NH_3)_2]$ with self-complementary 14-base-pair duplexes, the rate constant for forming an −AG− intrastanded cross-linked adduct is 50-fold higher than that for forming a −GA− adduct.[79] Moreover, the AG sequence was found to be platinated about two times faster than the GA sequence, irrespective of the cisplatin forms used (dichlorido, chloridoaqua, or diaqua), pH (3.8 or 7), and incubation time (16 or 64 h at 298 K) in an intramolecular competition experiment where TTAGTT and TTGATT groups were placed at identical distances from one extremity of a 19 base-pair radiolabeled DNA duplex.[81] The −AG− cross-links account for 20−25% of the total platinated DNA adducts formed by the reactions of *cis*-$[PtCl_2(NH_3)_2]$ and $[PtCl_2(en)]$ with salmon-sperm DNA, while no −GA− cross-linking products are detected.[7,8]

In duplex DNA, N3−H of T is H bonded to A and inaccessible to metal ions, so T is likely to be accessible only in single-stranded DNA and G-quadruplex DNA[41−43,45] or if there is T-base flipping out from the double helix.[40,82] Such DNA, for example, the human telomere-containing T2AG3 motifs, plays important roles in cell proliferation and apoptosis. The 3′-end of human telomere is not only G rich but also T rich, and the thymine bases are often located at the single-stranded loops when this region folds into G-quadruplex; the N3 sites are therefore accessible for metal attack.[83] Combined with exonuclease BSP digestion, in this present work mass spectrometry analysis revealed that the thymine bases T_{17} and T_{18} in the 22-mer human telomeric sequence **X** (5′-AGGGTTAGGGTTAGGGT$_{17}$T$_{18}$AGGG-3′) are not only kinetically but also thermodynamically competitive with the guanine bases G_9, G_{10}, G_{14}, G_{15}, G_{19}, and G_{20} for binding to complex **1** (Table 4 and Figure 6). Reaction of complex **1** with a 5-fold excess of the G4-**X** afforded thermodynamically stable T-bound ruthenated adducts for which the content increased with increasing reaction time, while the content of G-bound adducts did not markedly change with increasing time after 12 h of reaction. These indicate that thymine bases on the flexible loops of G-quadruplex DNA are more competitive with guanine bases. Here, in G-quadruplex DNA, N7 forms a hydrogen bond with N2H of another guanine, enhancing the competiveness of T N3 versus G N7. Considering the antiparallel G-quadruplex conformation,[44] the biphenyl ring of complex **1** may stack with the outermost G tetrads[31] to stabilize the G4 structure and favor coordination of ruthenium to thymine in the loop. Pt is known to have a strong preference for binding to guanine over adenine,[70,74,84,85] and the first platinum attack to a linear DNA sequence occurs always at a guanine.[5,12,13] However, the first platination occurs on adenine when *cis*-$[Pt(NH_3)_2(H_2O)_2](NO_3)_2$ and *trans*-$[Pt(NH_3)_2(H_2O)_2](NO_3)_2$ react with human telomeric G-quadruplex DNA in which the guanine bases form Hoogsteen hydrogen bonds and is then followed by chelation with a close adenine or a more nucleophilic guanine from the adjacent tetrad.[47] For monofunctional platinum complex PT-ACRAMTU (ACRAMTU = 1-[2-(acridin-9-ylamino)ethyl]-1,3-dimethylthiourea), the adenines in telomeric DNA are highly susceptible to platination and binding to A-N7 is kinetically favored over G-N7.[52] The unprecedented reactivity of complex **1** to T bases in G-quadruplex DNA again provides evidence for the distinct difference in binding preference of (arene)Ru(en) complexes and Pt-based complexes to DNA. It is notable that when the concentration of complex **1** increased, more ruthenium binds to guanine bases in G4 DNA, perhaps due to unfolding of the G-quadruplex DNA, which in turn leads to migration of T-bound ruthenium fragments to guanines, as observed for binding of complex **1** to single-stranded oligonucleotides **I**−**IV**.

We have recently shown that the intracellular concentration of ruthenium is about 320 pmol/10^6 cells after incubating human breast cancer MCF-7 cells with 20 μM of complex **1** at 310 K for 24 h.[56] As 10^6 cells contain ca. 10 μg of RNA and 5 μg of DNA, this corresponds to a G and T concentration of ca. 0.01 μmol/10^6 cells which is ca. 31-fold as much as the intracellular Ru (320 pmol/10^6 cells). This implies that inside cells the molar ratio of complex **1** to nucleobases (e.g., G and T) is very low. Therefore, the highly competitive ability of thymines versus guanines in G4-**X** for binding to complex **1** when the molar ratio of **1** to **X** was low suggests that binding to thymines in telomeric DNA may play an important role in the action of this class of ruthenium arene anticancer complexes.

■ CONCLUSION

The organometallic ruthenium arene anticancer complexes $[(\eta^6\text{-arene})Ru(en)Cl]^+$ (en = ethylenediamine) have been shown to bind to guanine bases selectively in natural DNA and synthetic single/double-stranded oligonucleotides, forming thermodynamically stable G-bound ruthenated DNA adducts. In this work, we demonstrated for the first time that thymine bases in 15-mer single-stranded oligonucleotides 5′-

CTCTCTX$_7$G$_8$Y$_9$CTTCTC-3′, where X = Y = T (**I**), X = C, Y = A (**II**), X = A, Y = T (**III**), and X = T, Y = A (**IV**), are kinetically competitive with guanine bases for binding to [(η^6-biphenyl)Ru(en)Cl]$^+$ (**1**). The T-bound ruthenated oligonucleotides eventually convert to diruthenated adducts via a second step of binding at G and to G-bound ruthenated species through dissociation of Ru from T. Moreover, binding of complex **1** to T$_7$ or T$_{11}$ in strand **I** exhibits positive cooperativity with the second step of binding to G$_8$ to form diruthenated adducts, while initial G$_8$ binding significantly retards further ruthenation at T bases. However, such a synergetic effect of T binding on G binding is weakened when the neighboring bases of G$_8$ are varied from T to A or C in strands **II**–**IV**. Further kinetic studies on reactions of complex **1** with dinucleotides have also confirmed the competitive ability of T binding compared to G. Moreover, kinetic interactions of complex **1** with 7-mer single-thymine-containing oligonucleotides indicate that the ruthenium complex preferentially binds to the middle T in the strands rather than to a T at the termini and to a T on the 5′-side of G rather than to the T on the 3′-side of G. These findings suggest that the sequence of DNA determines the preference for binding of ruthenium arene complexes to DNA and the competition between thymines and guanines for Ru binding.

Importantly, our studies reveal that the thymine bases in the loop of a human telomeric G-quadruplex sequence containing T2AG3 repeats are more competitive with guanine bases for binding to complex **1**. The amount of T-bound G-quadruplex adducts formed by **1** increases with extension of reaction time, leading to formation of thermodynamically stable T-bound G-quadruplex adducts. Taking into account the prevalence of G-quadruplex DNA in the human genome, in particular, in telomeres and promoters throughout the human genome,[86−88] the competition between thymine and guanine bases in G-quadruplex DNA for binding to the ruthenium arene anticancer complexes is worthy of further investigation. These findings also emphasize that kinetic studies and elucidation of reaction pathways for metallodrugs may provide insight into the mechanisms of anticancer activity since kinetic intermediates may play roles in biological signaling pathways.

■ ASSOCIATED CONTENT

Supporting Information

HPLC, MS, and kinetic data. This material is available free of charge via the Internet at http://pubs.acs.org.

■ AUTHOR INFORMATION

Corresponding Author

*E-mail: fuyi.wang@iccas.ac.cn (F.Y.W.); p.j.sadler@warwick.ac.uk (P.J.S.).

Author Contributions

$^{\perp}$K.W. and S.Y.L. contributed equally to this work.

Notes

The authors declare no competing financial interest.

■ ACKNOWLEDGMENTS

We thank NSFC (Grant Nos. 21020102039, 21135006, 21127901, 21275148 (Q. L.), and 21321003), the 973 Program of MOST (2013CB531805), the Innovation Method Fund of China (2012IM030400), and ERC (grant 247450) for support and Professor Yangzhong Liu at the University of Science and Technology of China for helpful discussions on calculation of kinetic constants.

■ REFERENCES

(1) Guo, Z. J.; Sadler, P. J. *Angew. Chem., Int. Ed.* **1999**, *38*, 1513−1531.
(2) Rosenberg, B.; Vancamp, L.; Krigas, T. *Nature* **1965**, *205*, 698−699.
(3) Bosl, G. J.; Motzer, R. J. *N. Engl. J. Med.* **1997**, *337*, 242−253.
(4) Jamieson, E. R.; Lippard, S. J. *Chem. Rev.* **1999**, *99*, 2467−2498.
(5) Jung, Y.; Lippard, S. J. *Chem. Rev.* **2007**, *107*, 1387−1407.
(6) Wang, D.; Lippard, S. J. *Nat. Rev. Drug Discovery* **2005**, *4*, 307−320.
(7) Eastman, A. *Biochemistry* **1986**, *25*, 3912−3915.
(8) Fichtinger-Schepman, A. M. J.; van der Veer, J. L.; den Hartog, J. H. J.; Lohman, P. H. M.; Reedijk, J. *Biochemistry* **1985**, *24*, 707−713.
(9) Kartalou, M.; Essigmann, J. M. *Mutat. Res.* **2001**, *478*, 1−21.
(10) Kartalou, M.; Essigmann, J. M. *Mutat. Res.* **2001**, *478*, 23−43.
(11) Alessio, E.; Mestroni, G.; Bergamo, A.; Sava, G. *Curr. Top. Med. Chem.* **2004**, *4*, 1525−1535.
(12) Bruijnincx, P. C. A.; Sadler, P. J. *Curr. Opin. Chem. Biol.* **2008**, *12*, 197−206.
(13) Kozelka, J. *Inorg. Chim. Acta* **2009**, *362*, 651−668.
(14) Dyson, P. J.; Sava, G. *Dalton Trans.* **2006**, 1929−1933.
(15) Galanski, M.; Arion, V. B.; Jakupec, M. A.; Keppler, B. K. *Curr. Pharm. Des.* **2003**, *9*, 2078−2089.
(16) Hambley, T. W. *Dalton Trans.* **2007**, 4929−4937.
(17) Storr, T.; Thompson, K. H.; Orvig, C. *Chem. Soc. Rev.* **2006**, *35*, 534−544.
(18) Gasser, G.; Ott, I.; Metzler-Nolte, N. *J. Med. Chem.* **2011**, *54*, 3−25.
(19) Hartinger, C. G.; Dyson, P. J. *Chem. Soc. Rev.* **2009**, *38*, 391−401.
(20) Meggers, E. *Chem. Commun.* **2009**, 1001−1010.
(21) Yan, Y. K.; Melchart, M.; Habtemariam, A.; Sadler, P. J. *Chem. Commun.* **2005**, 4764−4776.
(22) Aird, R. E.; Cummings, J.; Ritchie, A. A.; Muir, M.; Morris, R. E.; Chen, H.; Sadler, P. J.; Jodrell, D. I. *Br. J. Cancer* **2002**, *86*, 1652−1657.
(23) Chen, H. M.; Parkinson, J. A.; Parsons, S.; Coxall, R. A.; Gould, R. O.; Sadler, P. J. *J. Am. Chem. Soc.* **2002**, *124*, 3064−3082.
(24) Morris, R. E.; Aird, R. E.; Murdoch, P. D.; Chen, H. M.; Cummings, J.; Hughes, N. D.; Parsons, S.; Parkin, A.; Boyd, G.; Jodrell, D. I.; Sadler, P. J. *J. Med. Chem.* **2001**, *44*, 3616−3621.
(25) Wang, F. Y.; Habtemariam, A.; van der Geer, E. P. L.; Fernandez, R.; Melchart, M.; Deeth, R. J.; Aird, R.; Guichard, S.; Fabbiani, F. P. A.; Lozano-Casal, P.; Oswald, I. D. H.; Jodrell, D. I.; Parsons, S.; Sadler, P. J. *Proc. Natl. Acad. Sci. U.S.A.* **2005**, *102*, 18269−18274.
(26) Habtemariam, A.; Melchart, M.; Fernandez, R.; Parsons, S.; Oswald, I. D. H.; Parkin, A.; Fabbiani, F. P. A.; Davidson, J. E.; Dawson, A.; Aird, R. E.; Jodrell, D. I.; Sadler, P. J. *J. Med. Chem.* **2006**, *49*, 6858−6868.
(27) Sava, G.; Bergamo, A. *Int. J. Oncol.* **2000**, *17*, 353−365.
(28) Jakupec, M. A.; Galanski, M.; Arion, V. B.; Hartinger, C. G.; Keppler, B. K. *Dalton Trans.* **2008**, 183−194.
(29) Rademaker-Lakhai, J. M.; van den Bongard, D.; Pluim, D.; Beijnen, J. H.; Schellens, J. H. M. *Clin. Cancer Res.* **2004**, *10*, 3717−3727.
(30) Chen, H. M.; Parkinson, J. A.; Morris, R. E.; Sadler, P. J. *J. Am. Chem. Soc.* **2003**, *125*, 173−186.
(31) Liu, H. K.; Berners-Price, S. J.; Wang, F. Y.; Parkinson, J. A.; Xu, J. J.; Bella, J.; Sadler, P. J. *Angew. Chem., Int. Ed.* **2006**, *45*, 8153−8156.
(32) Liu, H. K.; Parkinson, J. A.; Bella, J.; Wang, F. Y.; Sadler, P. J. *Chem. Sci.* **2010**, *1*, 258−270.
(33) Liu, H. K.; Sadler, P. J. *Acc. Chem. Res.* **2011**, *44*, 349−359.
(34) Liu, H. K.; Wang, F. Y.; Parkinson, J. A.; Bella, J.; Sadler, P. J. *Chem.—Eur. J.* **2006**, *12*, 6151−6165.
(35) Novakova, O.; Chen, H. M.; Vrana, O.; Rodger, A.; Sadler, P. J.; Brabec, V. *Biochemistry* **2003**, *42*, 11544−11554.

(36) Novakova, O.; Kasparkova, J.; Bursova, V.; Hofr, C.; Vojtiskova, M.; Chen, H. M.; Sadler, P. J.; Brabec, V. *Chem. Biol.* **2005**, *12*, 121−129.
(37) Wang, F. Y.; Bella, J.; Parkinson, J. A.; Sadler, P. J. *J. Biol. Inorg. Chem.* **2005**, *10*, 147−155.
(38) Wang, F. Y.; Xu, J. J.; Habtemariam, A.; Bella, J.; Sadler, P. J. *J. Am. Chem. Soc.* **2005**, *127*, 17734−17743.
(39) Wu, K.; Hu, W. B.; Luo, Q.; Li, X. C.; Xiong, S. X.; Sadler, P. J.; Wang, F. Y. *J. Am. Soc. Mass Spectrom.* **2013**, *24*, 410−420.
(40) Klimasauskas, S.; Kumar, S.; Roberts, R. J.; Cheng, X. D. *Cell* **1994**, *76*, 357−369.
(41) Blackburn, E. H. *Nature* **1991**, *350*, 569−573.
(42) Smith, F. W.; Feigon, J. *Nature* **1992**, *356*, 164−168.
(43) Williamson, J. R.; Raghuraman, M. K.; Cech, T. R. *Cell* **1989**, *59*, 871−880.
(44) Wang, Y.; Patel, D. J. *Structure* **1993**, *1*, 263−282.
(45) Parkinson, G. N.; Lee, M. P. H.; Neidle, S. *Nature* **2002**, *417*, 876−880.
(46) Ishibashi, T.; Lippard, S. J. *Proc. Natl. Acad. Sci. U.S.A.* **1998**, *95*, 4219−4223.
(47) Redon, S.; Bombard, S.; Elizondo-Riojas, M. A.; Chottard, J. C. *Nucleic Acids Res.* **2003**, *31*, 1605−1613.
(48) Wang, F.; Chen, H. M.; Parsons, S.; Oswald, L. D. H.; Davidson, J. E.; Sadler, P. J. *Chem.—Eur. J.* **2003**, *9*, 5810−5820.
(49) *SCIENTIST*, 2.01 ed.; Micromath Scientific Software: Salt Lake City, UT, 1995.
(50) Coordination of Ru(II) complexes to ODNs had little effect on the extinction coefficients at 260 nm of ODNs (data not shown).
(51) Hudson, J. S.; Brooks, S. C.; Graves, D. E. *Biochemistry* **2009**, *48*, 4440−4447.
(52) Rao, L.; Bierbach, U. *J. Am. Chem. Soc.* **2007**, *129*, 15764−15765.
(53) Dapic, V.; Abdomerovic, V.; Marrington, R.; Peberdy, J.; Rodger, A.; Trent, J. O.; Bates, P. J. *Nucleic Acids Res.* **2003**, *31*, 2097−2107.
(54) Wu, K.; Luo, Q.; Hu, W. B.; Li, X. C.; Wang, F. Y.; Xiong, S. X.; Sadler, P. J. *Metallomics* **2012**, *4*, 139−148.
(55) We applied tandem mass spectrometry to identify the binding sites of the ruthenium complex **1** on a 7-mer oligonucleotide A_1G_2CCCCC. Results verified that complex **1** selectively bound to the G base, though the BSP digestion was found to be arrested at both A_1 and G_2 sites. Detailed results will be published elsewhere.
(56) Guo, W.; Zheng, W.; Luo, Q.; Li, X. C.; Zhao, Y.; Xiong, S. X.; Wang, F. Y. *Inorg. Chem.* **2013**, *52*, 5328−5338.
(57) Shionoya, M.; Kimura, E.; Shiro, M. *J. Am. Chem. Soc.* **1993**, *115*, 6730−6737.
(58) Kikuta, E.; Aoki, S.; Kimura, E. *J. Am. Chem. Soc.* **2001**, *123*, 7911−7912.
(59) Vinje, J.; Sletten, E.; Kozelka, J. *Chem.—Eur. J.* **2005**, *11*, 3863−3871.
(60) van der Wijst, T.; Guerra, C. F.; Swart, M.; Bickelhaupt, F. M.; Lippert, B. *Chem.—Eur. J.* **2009**, *15*, 209−218.
(61) Thewalt, U.; Neugebauer, D.; Lippert, B. *Inorg. Chem.* **1984**, *23*, 1713−1718.
(62) Keenea, F. R.; Smith, J. A.; Collins, J. G. *Coord. Chem. Rev.* **2009**, *253*, 2021−2035.
(63) Monjardet-Bas, V.; Elizondo-Riojas, M. A.; Chottard, J. C.; Kozelka, J. *Angew. Chem., Int. Ed.* **2002**, *41*, 2998−3001.
(64) Ramachandran, S.; Temple, B. R.; Chaney, S. G.; Dokholyan, N. V. *Nucleic Acids Res.* **2009**, *37*, 2434−2448.
(65) Legendre, F.; Kozelka, J.; Chottard, J. C. *Inorg. Chem.* **1998**, *37*, 3964−3967.
(66) Reeder, F.; Guo, Z. J.; Murdoch, P. D.; Corazza, A.; Hambley, T. W.; Berners-Price, S. J.; Chottard, J. C.; Sadler, P. J. *Eur. J. Biochem.* **1997**, *249*, 370−382.
(67) Reeder, F.; Gonnet, F.; Kozelka, J.; Chottard, J. C. *Chem.—Eur. J.* **1996**, *2*, 1068−1076.
(68) Hambley, T. W. *Dalton Trans.* **2001**, 2711−2718.
(69) Barnham, K. J.; Berners-Price, S. J.; Frenkiel, T. A.; Frey, U.; Sadler, P. J. *Angew. Chem., Int. Ed.* **1995**, *34*, 1874−1877.
(70) Martin, R. B. *Acc. Chem. Res.* **1985**, *18*, 32−38.
(71) Legendre, F.; Bas, V.; Kozelka, J.; Chottard, J. C. *Chem.—Eur. J.* **2000**, *6*, 2002−2010.
(72) Marzilli, L. G.; Kistenmacher, T. J. *Acc. Chem. Res.* **1977**, *10*, 146−152.
(73) Muller-Dethlefs, K.; Hobza, P. *Chem. Rev.* **2000**, *100*, 143−167.
(74) Bancroft, D. P.; Lepre, C. A.; Lippard, S. J. *J. Am. Chem. Soc.* **1990**, *112*, 6860−6871.
(75) Elmroth, S. K. C.; Lippard, S. J. *J. Am. Chem. Soc.* **1994**, *116*, 3633−3634.
(76) Sykfont, A.; Ericson, A.; Elmroth, S. K. C. *Chem. Commun.* **2001**, 1190−1191.
(77) Erkkila, K. E.; Odom, D. T.; Barton, J. K. *Chem. Rev.* **1999**, *99*, 2777−2795.
(78) Dewan, J. C. *J. Am. Chem. Soc.* **1984**, *106*, 7239−7244.
(79) Davies, M. S.; Berners-Price, S. J.; Hambley, T. W. *J. Am. Chem. Soc.* **1998**, *120*, 11380−11390.
(80) Mantri, Y.; Lippard, S. J.; Baik, M. H. *J. Am. Chem. Soc.* **2007**, *129*, 5023−5030.
(81) Riou, J. F.; Guittat, L.; Mailliet, P.; Laoui, A.; Renou, E.; Petitgenet, O.; Megnin-Chanet, F.; Helene, C.; Mergny, J. L. *Proc. Natl. Acad. Sci. U.S.A.* **2002**, *99*, 2672−2677.
(82) Priyakumar, U. D.; MacKerell, A. D. *Chem. Rev.* **2006**, *106*, 489−505.
(83) Neidle, S. *Curr. Opin. Struct. Biol.* **2009**, *19*, 239−250.
(84) Arpalahti, J.; Lippert, B. *Inorg. Chem.* **1990**, *29*, 104−110.
(85) Marcelis, A. T. M.; Erkelens, C.; Reedijk, J. *Inorg. Chim. Acta* **1984**, *91*, 129−135.
(86) Huppert, J. L.; Balasubramanian, S. *Nucleic Acids Res.* **2007**, *35*, 406−413.
(87) Todd, A. K.; Johnston, M.; Neidle, S. *Nucleic Acids Res.* **2005**, *33*, 2901−2907.
(88) Hershman, S. G.; Chen, Q.; Lee, J. Y.; Kozak, M. L.; Yue, P.; Wang, L. S.; Johnson, F. B. *Nucleic Acids Res.* **2008**, *36*, 144−156.